Effect of synthetic cannabinoids on spontaneous neuronal activity: evaluation using Ca^{2+} spiking and multi-electrode arrays

Tauskela, Joseph S.; Comas, Tanya; Hewitt, Melissa; Aylsworth, Amy; Zhao, Xigeng; Martina, Marzia; Costain, Willard J.

Publisher's version / Version de l'éditeur:
https://doi.org/10.1016/j.ejphar.2016.05.038
European Journal of Pharmacology, 2016-06-02

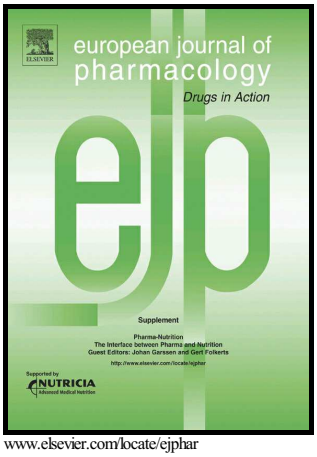

www.elsevier.com/locate/ejphar

Effect of synthetic cannabinoids on spontaneous neuronal activity: Evaluation using Ca^{2+} spiking and multi-electrode arrays

Joseph S Tauskela, Tanya Comas, Melissa Hewitt, Amy Aylsworth, Xigeng Zhao, Marzia Martina, Willard J Costain

PII: S0014-2999(16)30354-5
DOI: http://dx.doi.org/10.1016/j.ejphar.2016.05.038
Reference: EJP70665

To appear in: *European Journal of Pharmacology*

Received date: 22 February 2016
Revised date: 18 May 2016
Accepted date: 30 May 2016

Cite this article as: Joseph S Tauskela, Tanya Comas, Melissa Hewitt, Amy Aylsworth, Xigeng Zhao, Marzia Martina and Willard J Costain, Effect o synthetic cannabinoids on spontaneous neuronal activity: Evaluation using Ca^{2} spiking and multi-electrode arrays, *European Journal of Pharmacology* http://dx.doi.org/10.1016/j.ejphar.2016.05.038

Effect of synthetic cannabinoids on spontaneous neuronal activity: Evaluation using Ca^{2+} spiking and multi-electrode arrays

Joseph S Tauskela*, Tanya Comas, Melissa Hewitt, Amy Aylsworth, Xigeng Zhao, Marzia Martina, Willard J Costain

Department of Translational Bioscience, Human Health Therapeutics, National Research Council Canada, 1200 Montreal Road, Ottawa, Ontario, Canada K1A 0R6

*Corresponding Author: joe.tauskela@nrc-cnrc.gc.ca

Abstract

Activation of cannabinoid receptor 1 (CB_1) inhibits synaptic transmission in hippocampal neurons. The goal of this study was to evaluate the ability of benchmark and emerging synthetic cannabinoids to suppress neuronal activity *in vitro* using two complementary techniques, Ca^{2+} spiking and multi-electrode arrays (MEAs). Neuron culture and fluorescence imaging conditions were extensively optimized to provide maximum sensitivity for detection of suppression of neural activity by cannabinoids. The neuronal Ca^{2+} spiking frequency was significantly suppressed within 10 min by the prototypic aminoalkylindole cannabinoid, WIN 55,212-2 (10 μM). Suppression by WIN 55,212-2 was not improved by pharmacological intervention with signaling pathways known to interfere with CB_1 signaling. The naphthoylindole CB_1 agonist, JWH-018 suppressed Ca^{2+} spiking at a lower concentration (2.5 μM), and the CB_1 antagonist rimonabant (5 μM), reversed this suppression. In the MEA assay, the ability of synthetic CB_1 agonists to suppress spontaneous electrical activity of hippocampal neurons was evaluated over 80 min sessions. All benchmark (WIN 55,212-2, HU-210, CP 55,940 and JWH-018) and emerging synthetic cannabinoids (XLR-11, JWH-250, 5F-PB-22, AB-PINACA and MAM-2201) suppressed neural activity at a concentration of 10 μM; furthermore, several of these compounds also significantly suppressed activity at 1 μM concentrations. Rimonabant partially reversed spiking suppression of 5F-PB-22 and, to a lesser extent, of MAM-2201, supporting CB_1-mediated involvement, although the inactive WIN 55,212-3 also partially suppressed activity. Taken together, synthetic cannabinoid CB_1-mediated suppression of neuronal activity was detected using Ca^{2+} spiking and MEAs.

Keywords: Cannabinoid receptor 1, neuron, Ca^{2+} spiking, multielectrode array, 'spice' compounds

Chemical compounds studied in this article

AB-PINACA (PubMed CID: 71301472); CP 55,940 (PubMed CID: 104895); HU-210 (PubMed CID: 9821569); JWH-018 (PubMed CID: 10382701); JWH-250 (PubMed CID: 44397540); MAM-2201: (PubMed CID: 66570720); rimonabant: (PubMed CID: 104850); WIN 55,212-2 (PubMed CID: 5311501); XLR-11: (PubMed CID: 57501498)

1.0 Introduction

Products containing synthetic cannabinoids, notably the herbal blends Spice, are increasingly being used recreationally, potentially causing toxicity not associated with the principal psychoactive component of marijuana, Δ(9)-tetrahydrocannabinol (Δ^9-THC) (Brents and Prather, 2014; Wiley et al., 2011; Seely et al., 2012). A growing array of structurally diverse emerging synthetic cannabinoids (ESCs) has increased the burden of regulatory and law enforcement agencies, precipitating an urgent need to understand synthetic cannabinoid pharmacology. We have recently shown that ESCs display high potency and efficacy at the CB_1 of HEK293 cells transfected with this receptor (Costain et al., 2015). It is important that ESCs identified as CB_1 agonists also display agonist activity against native receptors, so our interest is in optimizing assays aimed at confirming that ESCs display agonist activity in neuron assemblies.

CB_1 are highly expressed in GABAergic terminals of the forebrain, causing inhibition of GABA release, but CB_1 are also located on axons of glutamatergic neurons in the hippocampus and cortex; activation of CB_1 by cannabinoids inhibits glutamatergic synaptic transmission in hippocampal neurons primarily by causing inhibition of pre-synaptic glutamate release (Kawamura et al., 2006; Ohno-Shosaku et al., 2002; Domenici et al., 2006). Reduction of Mg^{2+} to 0.1 mM ('low' Mg^{2+} treatment) in extracellular buffer bathing cultured hippocampal neurons increases the frequency of transient increases in cytoplasmic Ca^{2+} levels (Ca^{2+} spiking), in a manner which depends on glutamatergic neurotransmission and CB_1 agonists suppress Ca^{2+} spiking (Shen et al., 1996). Different classes of cannabinoids can suppress neuronal Ca^{2+} spiking,

although with differing efficacy and potency: these classes include endocannabinoids (those produced endogenously in the brain), Δ^9-THC, and synthetic cannabinoids (those produced in laboratories through chemical synthesis, some of which are controlled substances) (Shen et al., 1996; Shen and Thayer, 1998b; Shen and Thayer, 1999; Blair et al., 2006; Deshpande et al., 2007; Pacico and Mingorance-Le, 2014). Such commonality in pharmacology between cannabinoid classes suggests consistency in the pre-synaptic based mechanism of inhibition of excitatory neurotransmission.

A more recent complementary tool for neuropharmacological assessment is the multi-electrode array (MEA), which allows for a non-invasive electrophysiological interrogation of neuron preparations grown over arrays of planar microelectrodes. Action potentials may be asynchronous among neurons in the network, but are often synchronous for the duration of the culture, leading to network-wide electrical discharges known as bursts, with larger bursts correlating with Ca^{2+} spikes (Cao et al., 2012; Jimbo et al., 1993). Hence, MEAs allow investigation of the functions which govern neural electrical activity.

The objective was to determine if ESCs display the same ability as benchmark synthetic cannabinoids to suppress spontaneous Ca^{2+} spiking and electrical activity using primary hippocampal neurons plated on MEAs. Due to an unanticipated lower potency of a benchmark cannabinoid WIN 55,212-2 in suppressing Ca^{2+} spiking, extensive effort was devoted to optimization of culturing and imaging methodology, evaluation of potential interference by other GPCR-mediated signaling, and the effect of a CB_1 antagonist rimonabant. These optimized conditions for Ca^{2+} spiking technique were used to evaluate 4 benchmark and 5 ESCs, which is reported in a companion study (Costain et al., 2015). Second, we evaluated whether these 9 cannabinoids suppressed electrical activity in MEAs.

2.0 Materials and Methods

2.1 Materials

Tissue culture plates were purchased from Du Pont-Life Technologies (Burlington, ON, Canada) or VWR Canlab (Mississauga, ON, Canada). Fetal bovine serum and horse serum were bought from Gemini Bio (Woodland, CA, U.S.A.) and Hyclone Laboratories (Logan, UT, U.S.A.), respectively. Minimal essential medium (MEM) was obtained from Wisent Canadian Laboratories (St-Bruno, QC, Canada). Fluo-4-AM was bought from Molecular Probes (Eugene,

OR, U.S.A.). (+)-WIN 55,212-2, (-)-CP 55,940, rimonabant (SR141716) were purchased from Cayman Chemical (Ann Arbor, MI, USA). HU-210 and JWH-018 were purchased from Toronto Research Chemicals Inc. (Toronto, ON, Canada). JWH-250, XLR-11, AB-PINACA, MAM-2201, and 5F-PB-22 were generously provided by the Canadian Border Services Agency. WIN 55,212-3 was purchased from Tocris Bioscience. N-methyl-D-aspartate (NMDA), tetrodotoxin (TTX), CGP 55845, baclofen, theophylline, 8-cyclopentyl-1,3-dipropylxanthine (DPCPX) and all other reagents were purchased from Sigma (St. Louis, MO, U.S.A.).

2.2 Ca^{2+} spiking experiments

2.2.1 Cortical or hippocampal neuron cultures

Cultures of E18 rat cortical or hippocampal neurons were prepared based on a previous procedure (Tauskela et al., 2003). Timed-pregnant Sprague-Dawley rats (Charles River Canada, St. Constant, QC, Canada) were anesthetized with 4% isofluorane and killed by cervical dislocation. Following dissection of the cortical and hippocampal region of the fetal brain, the tissue was centrifuged at 1000 *g* for 3 min at 4 °C and then dispersed by trituration. Plating densities for hippocampal or cortical neuron cultures were either 0.35 x 10^6 (low density), 0.65 x 10^6 (medium density) or 1.3 x 10^6 (high density) cells/ml. Cells were plated on poly-L-lysine (PLL) coated glass coverslips in 24-well plates maintained in a standard incubator at 37 °C and 5% CO_2. Medium consisted of Eagle's minimal essential medium (EMEM) supplemented with 25 mM glucose, 10% fetal bovine serum and 10% horse serum. Cultures were treated with 30 µg/ml of 5-fluoro-2'-deoxyuridine and 70 µg/ml uridine after 4 days *in vitro* (DIV) to minimize glial growth, although astrocytes remained. As a further precaution to minimize microglia, cultures were flushed with a basic salt solution (see section 2.2.3) and cell culture medium was filtered (0.22 micron pore size) at 4 and 7 DIV and twice a week thereafter. At 7 DIV, 50% of the medium was replaced with medium consisting of EMEM plus 25 mM glucose and 10% horse serum and, at 14 and 16 DIV, this replacement volume decreased to 33%. Sterile water was added daily to maintain an osmolality range of 300-320 mOsmol. Experiments were performed on cultures growing from 14-25 days *in vitro*. The use of animals was approved by the Animal Care Committee of Human Health Therapeutics at the National Research Council Canada.

2.2.2 Hippocampal neurons plated on a pre-established astrocyte cell layer

Cortical/hippocampal neuron cultures were first established in 100mm dishes and maintained as described above. At 14 DIV, all neurons were killed by exposure to 100 μM NMDA for 40 min. Neuronal debris were washed with conditioned medium 1 and 4 days later, at which point only astrocytes remained adhered to the dish. At 18 DIV astrocytes were removed by a scraper, pelleted by centrifugation at 500 *g* for 3 min, mechanically dispersed and plated on PLL-coated glass coverslips in 24-well plates and allowed to grow to confluence over a 3 day period. The procedures as described above for plating and maintaining hippocampal neurons were followed, except when plating, media was removed and hippocampal neurons were plated at densities of 0.1×10^6 (very low density), 0.2×10^6 (low density) or 1.3×10^6 (high density) cells/ml.

2.2.3 Fluorescence imaging

Cultures were loaded with a Ca^{2+}-sensitive dye, 2.5 μM fluo-4-AM, for 30 min at room temperature in a balanced salt solution (BSS) with the following composition (in mM): 140 NaCl, 5 KCl, 2 $CaCl_2$, 20 HEPES, 3 glucose, 0.8 $MgCl_2$, 0.03 glycine, pH 7.4. Cultures were then allowed to recover for 30 min and experiments were performed within the next 2 h. Coverslips were mounted in a chamber on the microscope stage and Ca^{2+} spiking was induced by incubating the cultures at room temperature with a modified (low Mg^{2+}) HEPES buffered Hank's salt solution (HHSS) (in mM): 20 HEPES, 137 NaCl, 5 KCl, 1.3 $CaCl_2$, 0.1 $MgCl_2$, 0.4 KH_2PO_4, 0.6 Na_2HPO_4, 3 $NaHCO_3$, 0.01 glycine, pH 7.4, with 0.5% BSA present to minimize nonspecific absorption and to maximize solubility of the lipophilic cannabinoids (Kawamura et al., 2006) temperature. Following a 10 min equilibration period, intracellular Ca^{2+} levels were monitored by acquiring fluorescent images every 1.0 s. The excitation source was delivered through a Lambda DG-5 shutter instrument (Sutter Instrument Co, Novato, CA, USA) housing a Zeiss Axiovert 200 inverted microscope (ex 480 ± 15 nm and em 535 ± 20 nm) equipped with a 20 x objective, with images captured using a low light sensitivity Retiga Exi camera (QImaging, Burnaby, BC, Canada).

Due to variability in Ca^{2+} spiking frequency between coverslips, each coverslip served as its own internal control. Raw fluorescence intensity values were obtained from image stacks by selecting neuronal soma as regions of interest (ROIs) and quantitating average ROI intensity

using ImageJ. The raw data were then analyzed using an "in house" peak quantitation Matlab script (CaSpike; available on request), which extracts spike frequency for the pre- and post-drug periods. The percent inhibition of a drug was calculated as the ratio of post-drug to pre-drug Ca^{2+} spiking frequencies within the same coverslip. For each drug, images were acquired from a minimum of 5 coverslips, from at least 2 different platings, with a minimum of 9 arbitrarily selected neurons from each coverslip analyzed.

2.2.4 Drug Application

Two different methods of drug delivery to the imaging chamber were evaluated. For microperfusion experiments, drugs were delivered at a flow rate of 1 ml/min. For 'static' experiments, 50% of the HHSS in the recording chamber was replaced with HHSS containing a drug(s) at twice the desired final concentration. All cannabinoids were prepared in DMSO, with the exception of CP 55,940 which was prepared in methanol. $GABA_A$, $GABA_B$ and adenosine agonists or antagonists were also dissolved in DMSO, with the exception of baclofen which was dissolved in distilled water. The final concentration of solvent in aqueous solution was $\leq 0.2\%$.

2.3 Multi-electrode Array (MEA) experiments

2.3.1 Preparation of Hippocampal Neuron Cultures

Hippocampal neurons were plated at 1.8×10^6 (high density) on PLL/laminin-coated 60-microelectrode dishes (ALA Scientific, Germany), and medium also contained 1% penicillin and streptomycin. Only cultures that exhibited a dense, homogenous monolayer of healthy neurons were retained for recordings. Cultures grown between 14-18 DIV were employed for recordings, from a minimum of 2 different platings. Each culture was exposed only once to a cannabinoid.

2.3.2 Recordings

For recording sessions, media was replaced with low (0.1 mM) Mg^{2+} HHSS and MEAs were capped with a sterile vented tissue culture lid (Blau et al., 2009) to maintain sterility and prevent hydration loss. An MEA dish was positioned on the headstage, which was transferred to an incubator maintained at 37 °C, and 20 min was allowed to elapse before commencing recording, in order to minimize movement-induced artifact signals (Wagenaar et al., 2006). Due to variability in spontaneous activity between MEAs (Wagenaar et al., 2006), each MEA served as its own internal control: two 20 min baseline recordings were performed prior to acquiring

four 20 min recordings with a cannabinoid or DMSO vehicle present. We performed online extracellular spike detection using MC_RACK software (Multi Channel System), with a threshold set to ± 5 s.d. above the mean of the signal at each channel. Low frequency shifts in the raw signal were removed using a high pass filter with a cut-off frequency of 200 Hz. A significant source of error in the MEA analyses arises from variation in the responsiveness of individual electrodes on individual MEAs. A small number of the 59 electrodes were non-responsive, exhibiting low spontaneous spiking, which was likely due to low neuronal coverage. In order to identify and eliminate inactive electrodes, signal strength values were calculated for each electrode using the following equation:

$$S = abs\left(\frac{\bar{P_n} - d_n}{log_2(d_n/\bar{P_n}) * \bar{P_n}}\right)$$

where: S = signal strength; d_n = post-drug spike count; $\bar{P_n}$ = average of pre-drug spike count; n = electrode.

Plotting signal strength *versus* spike counts for individual post-drug recordings demonstrated a linear relationship between signal strength and spiking (**Fig. 1**). Electrodes with signal strength values below an empirically determined threshold were excluded from the dataset, so that subsequent calculations represented data derived from responsive electrodes only. Spike counts for each of the 4 sequential recordings performed in the presence of cannabinoid were normalized relative to the average spike count determined from the two pre-drug recordings. A minimum of 5 MEAs over a minimum of 2 different culture plating periods were employed for each condition.

2.3.3 Statistical Analyses

Data are presented as the mean ± S.E.M. Statistical comparisons were made by analysis of variance (ANOVA). When significant differences were observed, Dunnett's test was employed for multiple comparisons between vehicle column and other columns or Bonferroni's test was employed for multiple comparisons between columns. Statistical significance was inferred at $P < 0.05$.

3.0 Results

3.1 Ca^{2+} spiking

Assay conditions were optimized to allow maximal suppression of neuronal Ca^{2+} spiking frequency by the prototypic aminoalkylindole cannabinoid, WIN 55,212-2. Using 14-18 DIV cultures of hippocampal neurons plated at a high density (1.3×10^6 cells/ml), we first verified that Ca^{2+} spiking was stable, synchronous across neurons, susceptible to Na^+ channel blockade using TTX, and that the highest $[Ca^{2+}]_{in}$ achieved during spikes was sub-maximal, as verified by NMDA-induced maximal increases at the termination of the experiment (**Fig. 2**). Micro-perfusion of WIN 55,212-2 required a minimal 10 μM concentration in order to significantly suppress the Ca^{2+} spiking frequency (**Fig. 3A**; **Table 1**), representing approximately ~3 orders of magnitude lower potency than in the Thayer laboratory (Shen et al., 1996).

We evaluated different culture and fluorescence imaging conditions in an effort to improve the efficacy and potency of WIN 55,212-2 (**Table 1**), using practices in the Thayer laboratory as a guide (Shen et al., 1996). Introducing 10 μM WIN 55,212-2 via buffer replacement with a pipette (static) to hippocampal neuron cultures at the lowest possible density tested (0.35×10^6 cells/ml) resulted in the greatest suppression of spiking (**Fig. 3B; Table 1**), but 1 μM WIN 55,212-2 remained ineffective. One potential confounder could be astrocyte density, since astrocytes were less dense than in the Thayer laboratory (Shen and Thayer, 1998a). We found we could plate neurons at even lower densities on a previously established confluent astrocyte monolayer, a practice employed in the DeLorenzo laboratory (although they used postnatal DIV 2 hippocampal neurons (Deshpande et al., 2007)), while still yielding synchronous Ca^{2+} spiking: at a plating density 0.2×10^6 cells/ml, Ca^{2+} spiking was significantly suppressed by 10 μM WIN 55,212-2, but the pre-drug Ca^{2+} spiking frequency was considered unacceptably low (**Fig. 3D; Table 1**). Plating at even lower hippocampal neuron densities on an astrocyte bed resulted in asynchronous spiking between neurons (data not shown). WIN 55,212-2 did not suppress spiking in neurons plated at a high density on an astrocyte bed (Table 1). No improvement in the sensitivity of WIN 55,212-2 was detected when examining older cultures (21-25 DIV; data not shown), so all further work in this study employed 14-18 DIV cultures; at these ages, hippocampal neurons should be sufficiently mature that the CB_1 receptors distribute to a greater extent on processes than soma (3-4 weeks in culture) (Twitchell et al., 1997). Other Thayer laboratory practices considered (but rejected) were as follows: plating a 'droplet' of neurons (poorer long-term viability), and no mitotic inhibitor (microglia proliferation). Other

parameters considered which which did not improve the sensitivity of WIN 55,212-2 were as follows: examining WIN 55,212-2 from another commercial source, employing never-frozen DMSO stocks of cannabinoids, employing 0.9 mM Mg^{2+} (normal) or nominally Mg^{2+}-free HHSS and testing the high affinity Fura-2 and low-affinity Fluo-4FF Ca^{2+}-sensitive fluorescence dyes (data not shown). We also evaluated cortical neuron cultures (1.3×10^6 cells/ml plating density): under perfusion conditions, 10 µM WIN 55,212-2 significantly suppressed Ca^{2+} spiking, but not as much as in the optimized hippocampal cultures. Under static conditions, slightly better suppression was observed (**Fig. 3C; Table 1**). Lower plating densities of cortical neurons could not be examined due to poorer long-term viability (data not shown). Summarizing, optimal conditions include the use of hippocampal neurons plated at 0.35×10^6 cells/ml and the delivery of cannabinoids under static conditions, a protocol followed for the remainder of the study.

Non-cannabinoid neuron signal transduction events involving other G-protein coupled receptors have been shown to decrease the potency of WIN 55,212-2, albeit in outputs other than Ca^{2+} spiking. Therefore, we considered if the potency of WIN 55,212-2 could be improved by interfering or activating these pathways. $GABA_B$ receptors are $G_{i/o}$-coupled proteins and, in examining their role, the agonist baclofen (10 µM) completely suppressed Ca^{2+} spiking (**Fig. 4A**), which can be attributed to the depression of synaptic release of glutamate in cultured neurons (Obrietan and van den Pol, 1999). This raised the possibility that pre-synaptic $GABA_B$ receptors could interfere with cannabinoids in suppressing glutamate release, as reported in hippocampal slices (Messer and Levine, 2012), although not in another study (Hoffman et al., 2010). However, the $GABA_B$ receptor antagonist CGP 55845 (10 µM) did not significantly increase Ca^{2+} spiking frequency, implying minimal endogenous $GABA_B$ receptor activation (**Fig. 4A**). Moreover, testing WIN 55,212-2 (10 µM) with CGP 55845 present did not significantly suppress Ca^{2+} spiking relative to WIN 55,212-2 alone.

Given that CB_1 receptors are expressed more densely at inhibitory presynaptic terminals than at excitatory ones (Kawamura et al., 2006; Marsicano and Lutz, 1999), a high level of inhibitory tone may have counteracted action at excitatory terminals by WIN 55,212-2 (Messer and Levine, 2012). However, the $GABA_A$ receptor antagonist bicuculline (50 µM) did not significantly increase the Ca^{2+} spiking frequency, and the further addition of WIN 55,212-2 did

not significantly decrease spiking (**Fig. 4A** and **4C**), suggesting that endogenous $GABA_A$ergic activity did not influence the potency or efficacy of WIN 55,212-2.

Adenosine A_1 receptor activation eliminates CB_1-mediated inhibition of glutamate release, which can be prevented by adenosine A_1 receptor antagonists (Hoffman et al., 2010; Sousa, ssaife-Lopes et al., 2011). The adenosine receptor antagonist, theophylline (100 µM; **Fig. 4B**), and the more specific A_1 receptor antagonist, DPCPX (1 µM), each induced a significant increase in Ca^{2+} spiking frequency, consistent with endogenous receptor activation as a potent inhibitor of synaptic release in the (CA1) hippocampus (Dunwiddie and Masino, 2001). This raised the possibility that ongoing activation of pre-synaptic adenosine A_1 receptors could interfere with the ability of cannabinoids to suppress glutamate release. However, in the presence of either antagonist, WIN 55,212-2 (10 µM) did not significantly suppress Ca^{2+} spiking relative to WIN 55,212-2 alone. Taken together, a general deficit in the ability of G-protein coupled receptors to pre-synaptically modulate glutamate release cannot account for the lower potency of WIN 55,212-2, nor can cross-talk between adenosine A_1 receptors and CB_1 be responsible.

In an effort to more directly determine if CB_1 activation was involved, we determined if suppression of Ca^{2+} spiking in one of the most efficacious cannabinoids, JWH-018, could be reversed by the CB_1 antagonist rimonabant. In optimizing concentrations to be employed, a dose response analysis revealed that rimonabant alone significantly suppressed Ca^{2+} spiking at 10, but not 5 or 1, µM (**Fig. 5A**). However, administering 1 or 5 µM rimonabant before subsequent addition of 10 µM JWH-018 did not cause a significant inhibition of Ca^{2+} spiking. Therefore, we determined that the minimal concentration of JWH-018 that could suppress Ca^{2+}spiking was 2.5 µM (**Fig. 5B**), but not 1 µM (data not shown). Rimonabant (5 µM) did not reverse the ability of 5 µM JWH-018 to suppress spiking but did significantly reverse the ability of a lower concentration (2.5 µM) of JWH-018 to suppress Ca^{2+} spiking (**Figs. 5A and C**).

3.2 Multielectrode arrays (MEAs)

The suitability of MEA technology was established by investigating 4 benchmark and 5 ESCs. The optimized procedures developed for Ca^{2+} spiking experiments were also employed for MEAs, except hippocampal neurons were plated at high density, and spontaneous activity in 0.1 mM Mg^{2+} HHSS was monitored over a total 80 min exposure of a cannabinoid, in 20 min

recording sessions. Hippocampal cultures grown on MEA dishes typically displayed good coverage of neurons over nearly all microelectrodes (**Fig. 6A**), with several neurons typically in proximity to each microelectrode. In typical raster plots of activity, regular synchronous firing of neurons (network bursts) was detected from the majority of the 59 electrodes, as expected from the extensive neuronal coverage of electrodes. In a representative experiment, addition of 5F-PB-22 (10 μM) caused a profound decrease in spontaneous activity that was sustained over the subsequent 80 min recording session (**Fig. 6B**).

Recordings obtained in the presence of vehicle (DMSO) were used as a control for all comparisons (**Fig. 7A**). Overall, WIN 55,212-2 (10 μM) significantly suppressed spiking, but not for any time-matched points, while a 1 μM concentration did not significantly suppress spiking (**Fig. 7B**). In comparison, WIN 55,212-3 (10 μM) exerted an overall and time-matched significant suppression (**Fig. 7C**). The dibenzopyran derivative, HU-210 (10 μM), and the bicyclic, CP 55,940 (10 μM), displayed stronger suppressive effects with longer incubation times and overall suppression (**Fig. 7D-E**). JWH-018 (10 μM) showed significant suppression at all time points, and even at 1 μM displayed significant overall suppression, although not at any individual time-points (**Fig. 7F**). Taken together, except for WIN 55,212-2, the MEA methodology employed allowed for detection of suppression of spontaneous activity by benchmark synthetic cannabinoids.

In a separate publication (Costain et al., 2015), we demonstrated that five ESCs (10 μM) significantly suppressed hippocampal neuronal Ca^{2+} spiking. We evaluated the effect of these ESCs using MEA methodology. JWH-250 (10 μM) significantly suppressed spiking at all time points, while XLR-11 (10 μM) significantly suppressed activity at the latter 3 time-points, and each was overall significantly suppressive (**Figs. 8A and 8B, respectively**). AB-PINACA caused significant suppression overall at both 10 and 1 μM (**Fig. 8C**). MAM-2201 and 5F-PB-22 strongly suppressed activity at 10 μM at all individual time points, and demonstrated significant suppression overall at 1 μM (**Figs. 8D and 8E, respectively**). Hence, all ESCs produced significant, dose-dependent suppression over the duration of the experiment, and to varying degrees at time-matched points, with the greatest suppression observed at longer incubation times and higher concentrations.

We examined the ability of rimonabant to inhibit suppression for two ESCs. The maximal concentration of rimonabant which did not suppress spontaneous activity was 5 µM (**Fig. 9A**). The minimal concentration of MAM-2201 which suppressed activity at all time points was 5 µM (**Fig. 9B**). Using these concentrations, rimonabant reversed the suppression of activity caused by MAM-2201 for the first time-matched recording only (**Fig. 9B**). The minimal concentration of 5F-PB-22 which suppressed activity at all time points was 10 µM (**Fig. 9C**). Rimonabant significantly reversed 5F-PB-22-induced suppression of activity at the first three time-matched recordings and overall (**Fig. 9C**). Hence, efficacy of rimonabant in reversing the effect of these ESCs was most evident at early time points.

4.0 Discussion

This study confirmed that synthetic cannabinoids identified as CB_1 agonists in transfected cells demonstrate physiological effects in neurons containing native receptors. Adopting an assay in cultured hippocampal neurons (Shen et al., 1996), and employing a prototypical cannabinoid, WIN 55-212,2, as a benchmark, potency and efficacy was unexpectedly poor. A 10 µM concentration was required to significantly suppress Ca^{2+} spiking, despite abundant CB_1 expression in hippocampal neuron cultures in our laboratory (Costain et al., 2015). This raised concerns about the neuronal culture system, the fluorescence imaging methodology and CB_1-independent effects, which were systematically addressed. Efficacy but not potency was improved by extensive optimization of protocols for culturing neurons and Ca^{2+} imaging, some of which differed from the Thayer laboratory. Generally similar potency and efficacy was achieved between the using the Ca^{2+} spiking and MEA technique, both with several benchmark and (ESCs), although with differences in unique subsets of cannabinoids detected. This nonetheless implyed that technical capabilities were adequate to detect a neuro-suppressive effect of the cannabinoids. Pharmacological blockade of a panel of signal transduction pathways which could potentially to interfere with the WIN 55-212,2-CB_1 interaction did not improve its potency and efficacy. Thus, the basis for differences with the Thayer laboratory results is unknown, but it is noted that the levels of potency/efficacy detected here are similar with some laboratories (see below). The CB_1 receptor antagonist rimonabant significantly reversed suppression of Ca^{2+} spiking by another benchmark cannabinoid, JWH-018, confirming a CB_1-mediated component. Rimonabant also partially reversed suppression of electrical activity by 5F-

PB-22 and, to a lesser extent, MAM-2201. Moreover, the inactive enantiomer, 10 µM WIN 55-212,3, did not suppress Ca^{2+} spiking (Costain et al., 2015). Taken together, our analyses support a CB_1-mediated suppression of Ca^{2+} spiking and electrical activity by benchmark and emerging cannabinoids determined to be CB_1 agonists.

4.1 Optimization of the neuronal Ca^{2+} spiking and MEA assays to improve efficacy and potency

In the Ca^{2+} spiking assay, numerous approaches were considered. Only plating of hippocampal neurons at a low density (0.35 million cells/ml) and pipette delivery of WIN 55,212-2 improved efficacy (Table 1). Low neuronal density appears to be common with the most relevant studies (Shen et al., 2007). Sparser hippocampal neuron cultures exhibit simpler dendritic trees and fewer dendritic spines, with more synapses on dendritic shafts, so fewer pre-synapses may result in stronger connections between neurons (Ivenshitz and Segal, 2010). The improvement observed with pipette delivery was independent of spiking frequency (Table 1). Blocking $GABA_A$ receptors did not improve WIN 55,212-2 sensitivity (Fig. 4), which is consistent with another study (Messer and Levine, 2012). The Thayer group also reported WIN 55,212-2 did not affect inhibitory synaptic transmission (Shen et al., 1996). $GABA_B$ or adenosine A_1 receptors did not affect WIN 55,212-2 sensitivity (Fig. 4), in contrast to other reports examining a variety of experimental configurations and neuronal preparations (Hoffman et al., 2010; Sousa, ssaife-Lopes et al., 2011). An important goal for employing MEAs was to take advantage of its unique capabilities to improve detection of suppression of neural activity by cannabinoids. MEA technology allows much more sensitive detection of ion channel activity and not only Ca^{2+} receptors, in a noninvasive manner (no Ca^{2+} dyes) over longer periods of interrogation (h versus min). All nine cannabinoids significantly suppressed activity at 10 µM concentrations in MEAs, while mostly subsets (three for Ca^{2+} spiking and four for MEAs) suppressed activity at 1 µM. Taken together, the extensive optimization of procedures, the lack of influence of other GPCR-mediated signaling, and the similarity in the requirement for 1-10 µM concentrations of cannabinoids to suppress neural activity in both fluorescence imaging and electrophysiological techniques, suggests attainment of the limit of detection.

The efficacy/potency of WIN 55,212-2 in suppressing neural activity considerably varies between laboratories. The Thayer group reported complete suppression of Ca^{2+} spiking at 0.1

μM (EC_{50} = 1.2 ± 0.7 nM) and of EPSCs at nM concentrations (Shen et al., 1996). However, closer to our experience, 5 μM WIN 55,212-2 was required to completely suppress low Mg^{2+}-induced status epilepticus (EC_{50} = 1.5 μM) (Deshpande et al. 2007), or for silencing of presynaptic nerve terminals (Ramirez-Franco et al., 2014). WIN 55,212-2 (10 μM; lower concentrations were not reported) suppressed Ca^{2+} spiking in cultured cortical neurons (Pacico and Mingorance-Le, 2014). Depolarization (veratridine)-mediated release of L-glutamic acid in cortical neuron cultures required a relatively high WIN 55,212-2 concentration (IC_{50} = 12.2 μM) (Nicholson, Liao et al., 2003). WIN 55,212-2 (5 μM) suppresses hippocampal field potentials in 0 Mg^{2+} perfusate, but loses this ability in high extracellular potassium, and is restored at 30 μM, in a rimonabant-sensitive manner (Messer and Levine, 2012). Studies in slice preparations show considerable variable suppression of excitatory transmission but better potency at submicromolar EC_{50}'s and reversal by CB_1 receptor antagonists (Bajo et al., 2009; Hoffman et al., 2005; Kang-Park et al., 2007; Kawamura et al., 2006).

4.2 Mechanism of inhibition of neural activity

A CB_1-mediated mechanism is implicated since 5 μM rimonabant reversed suppression of neural activity by JWH-018 (Ca^{2+} spiking assay), and for 10 μM MAM-2201 and 5F-PB-22 at earlier time points (MEA assay). Rimonabant might have been less effective in this latter assay due to its 2-fold lower relative concentration relative to the agonist. Rimonabant (≤ 1 μM) completely reversed suppression of Ca^{2+} spiking in cultured hippocampal neurons induced by WIN 55,212,2 at concentrations of 100 nM (Shen and Thayer, 1998a) and even at 5 μM (Lauckner et al., 2005; Blair et al., 2006), as well as by Δ^9-THC (100 nM) (Shen and Thayer, 1999) and by the endocannabinoid 2-arachidonyl glycerol (1 μM) (Kelley and Thayer, 2004). Rimonabant exerts off-target effects (Pertwee, 2010), such as antagonism of mu-opioid receptors (Seely et al., 2012), which may preclude definitive interpretations.

The requirement for 10 μM WIN 55-212,2 to suppress neural activity in our hands raises the possibility of an additional non-CB_1 mediated component. Of most relevance, the Thayer laboratory reports that > 1 μM WIN 55-212,2 directly inhibits Ca^{2+} channels and that the inactive stereoisomer, WIN 55,212-3 (3 μM), inhibits 78 ± 13 % of Ca^{2+} spiking (Shen and Thayer, 1998b). However, we found that 10 μM WIN 55,212-3 did not suppress Ca^{2+} spiking (Costain et

al., 2015). Importantly, this suggests that WIN 55-212,2 suppresses Ca^{2+} channels at much higher concentrations in our neuron cultures than in the Thayer laboratory. Several plausible explanations exist. Cannabinoids may be less effective at blocking N- and P/Q-type voltage gated Ca^{2+} channels (VGCCs) (Twitchell et al., 1997; Shen and Thayer, 1998b; Sullivan, 1999), Na^{+} channels (Nicholson et al., 2003) or at inducing presynaptic silencing in our preparations (Pacico and Mingorance-Le, 2014; Ramirez-Franco et al., 2014). Other possibilities for variable efficacy/potency of cannabinoids between laboratories include: a lower CB_1 density in glutamatergic principal neurons relative to GABAergic interneurons (Marsicano and Lutz, 1999), differing G protein selectivity (Glass and Northup, 1999; Prather et al., 2000), less efficient coupling to G proteins in glutamatergic compared to 'GABAergic' CB_1 (Steindel et al., 2013), altered CB_1 trafficking to axonal plasma membranes (Leterrier et al., 2006), CB_1 desensitization (Kouznetsova, Kelley et al., 2002), CB_1 receptor internalization (Atwood et al., 2010) or interference by CB_2 receptor signaling (WIN 55,212-2 and JWH-018 are also agonists of CB_2 (Rajasekaran et al., 2013)). Some effects on neuronal activity by WIN 55,212,2 and other cannabinoids persist in the presence of CB_1 antagonists or with genetic ablation of CB_1 (reviewed in (Kreitzer and Stella, 2009; Pertwee, 2010)). However, a study showing that WIN 55,212-2 (1 µM) decreases excitatory neurotransmission in CB_1 knockout animals (Ohno-Shosaku et al., 2002) was not substantiated even at 5 µM (Domenici et al., 2006; Takahashi and Castillo, 2006). Some studies suggest that a concentration of WIN 55,212-2 up to 5 µM exerts its actions solely at the CB_1 receptor (Bajo et al., 2009; Kawamura et al., 2006; Takahashi and Castillo, 2006), although contradictory data has been published (Hajos and Freund, 2002; Nemeth et al., 2008; Kofalvi et al., 2003). Ultimately, the variability of CB_1-dependent and independent activity of cannabinoids on neurons likely results from the indirect and complex nature of this signal transduction pathway.

5.0 Conclusions

Both assays provided complementary utility in detecting neuro-suppressive effects on neuronal activity via the CB_1 receptor. The MEA dataset builds on Ca^{2+} spiking and single-cell electrophysiology by showing that neural network activity can be suppressed by cannabinoid CB_1 receptor agonists.

Table 1. Optimization of Assay for Maximal Suppression of Ca^{2+} Spiking by WIN 55,212-2

Neuron Culture	Plating Density (million cells/ml)	WIN 55,212-2 Delivery Method	WIN 55,212-2 Concentration (μM)	Initial Ca^{2+} spiking frequency (Hz)	% Ca^{2+} spiking frequency with WIN 55,212-2 (normalized)
hippocampal	1.30	Perfusion	0	0.083 ± 0.009	94.4 ± 3.5
			0.1	0.089 ± 0.029	88.7 ± 9.7
			1.0	0.097 ± 0.014	81.6 ± 6.3
			10.0 [a]	0.104 ± 0.016	65.6 ± 8.0*
hippocampal	1.30	Static	0	0.122 ± 0.031	95.5 ± 7.9
			10.0	0.107 ± 0.015	73.2 ± 13.1
hippocampal	0.65	Static [b]	0	0.076 ± 0.020	103.6 ± 4.9
			10.0	0.120 ± 0.018	91.9 ± 17.6
hippocampal	0.35	Static [b]	0	0.118 ± 0.012	101.1 ± 4.8
			1.0	0.098 ± 0.010	94.7 ± 12.9
			10.0	0.113 ± 0.016	37.3 ± 9.1*
cortical	1.30 [c]	Perfusion	0	0.118 ± 0.009	92.5 ± 2.5
			10	0.136 ± 0.016	55.5 ± 4.2*
cortical	1.30	Static	0	0.072 ± 0.005	109.7 ± 5.9
			10	0.050 ± 0.004	44.3 ± 8.2*
Hippocampal/ Astrocyte pre-layer [d]	1.3	Static	10	0.011 ± 0.005	101.3 ± 8.1
Hippocampal/ Astrocyte pre-layer [d]	0.2	Static	10	0.009 ± 0.001	65.2 ± 16.7

[a] Data displayed for 14-25 DIV; 20-25 DIV data was not significantly different from 14-18 DIV data, so datasets were combined.
[b] Perfusion could not be employed for hippocampal cultures plated at 0.65 or 0.30 million cells/ml due to neuron adherence issues.
[c] Cortical cultures plated at 0.65 or 0.30 million cells/ml did not display sufficient long-term viability to be examined.
[d] Hippocampal neurons were plated at the indicated density on a confluent monolayer of astrocytes plated 4 days earlier.

* significantly different ($P < 0.01$) from 0 µM WIN 55,212-2 counterpart condition

Fig. 1. Logarithmic plot (base 2) of signal strength for a post-drug MEA recording *versus* average pre-drug spike counts. Two pre-drug recordings were obtained and average pre-drug spike counts ($\bar{P}$) are plotted on the abscissa. Each data point represents an individual electrode on the MEA. The dashed line represents the empirically determined threshold value used to exclude data from electrodes with weak signals.

Fig. 2. Ca^{2+} spiking profile from individual neuronal soma.

Hippocampal neurons plated at high density and loaded with Fluo-4 were perfused with 0.1 mM Mg^{2+} in HHSS in the following order: drug-free, 1 µM TTX (Na^{+} channel blocker; negative control), drug-free washout and 50 µM NMDA (glutamate receptor agonist; positive control). Vertical scale represents neuronal Fluo-4 fluorescence and horizontal scale represents time. **Inset**: fluorescence intensities determined from two neuronal soma depicted in red and black tracings, demonstrating synchronous Ca^{2+} spiking.

Fig. 3. (i) Ca^{2+} spiking profiles (before and during exposure to 10 µM WIN 55,212-2) and (ii) corresponding phase-contrast image from different neuron culture paradigms.

- **(A)** Hippocampal neurons plated at 1.3×10^6 cells/ml, with WIN 55,212-2 delivered via micro-perfusion.
- **(B)** Hippocampal neurons plated at 0.35×10^6 cells/ml, with WIN 55,212-2 delivered under static conditions.
- **(C)** Cortical neurons plated at 1.3×10^6 cells/ml, with WIN 55,212-2 delivered under static conditions.
- **(D)** Hippocampal neurons plated at 0.2×10^6 cells/ml on a pre-established confluent astrocyte monolayer, with WIN 55,212-2 delivered under static conditions.

In the Ca^{2+} spiking profiles, the vertical scale represents neuronal Fluo-4 fluorescence and horizontal scale represents time. Breaks in spiking in (B)-(D) represent when signal acquisition was paused during WIN 55,212-2 addition. In the phase contrast images, arrows indicate individual neuronal soma and the scale bar represents 50 microns.

Fig. 4. Effect of non-cannabinoid GPCR-mediated signaling on efficacy of WIN 55,212-2 in suppressing Ca^{2+} spiking in hippocampal neuron cultures.

In hippocampal neurons plated at low density and loaded with Fluo-4, Ca^{2+} spiking was monitored before and after addition of 0.1 % DMSO vehicle; a $GABA_B$ receptor agonist, baclofen (10 µM); a $GABA_B$ receptor antagonist, CGP 55845 (10 µM) ± WIN 55,212-2 (10 µM); an adenosine A_1 receptor antagonist, theophylline (100 µM) ± WIN 55,212-2 (10 µM); an adenosine A_1 receptor antagonist, DPCPX (1 µM) ± WIN 55,212-2 (10 µM) or; a $GABA_A$ receptor antagonist, bicuculline (50 µM) ± WIN 55,212-2 (10 µM). **(A)** For each drug evaluated, images were acquired from a minimum of 5 coverslips, from at least 2 different platings, with a minimum of 9 neuronal soma arbitrarily selected from each coverslip for determination of Ca^{2+} spiking frequency. The % frequency was calculated relative to the pre-drug condition within the same coverslip. * $P < 0.05$ relative to vehicle (dotted line), was determined using a one-way ANOVA and Dunnett's multiple comparison test. The inclusion of drug (CGP, theophylline or DPCPX) with WIN 55 212-2 did not significantly ($P > 0.05$) decrease frequency relative to WIN 55 212-2 alone (dashed line; black bars denote inclusion of WIN 55 212-2), as determined using a one-way ANOVA and Bonferroni's multiple comparison test. **(B)** Representative Ca^{2+} spiking profile (static conditions) obtained from one coverslip to which theophylline (100 µM) and WIN 55,212-2 (10 µM) were added sequentially. **(C)** Representative Ca^{2+} spiking profile (static conditions) obtained from one coverslip to which bicuculline (50 µM) and WIN 55,212-2 (10 µM) were added sequentially. For (B) and (C), vertical scale represents Fluo-4 fluorescence and horizontal scale represents time. Breaks in spiking represent pauses in signal acquisition to allow for addition of drug.

Fig. 5. Effect of the CB_1 antagonist rimonabant on JWH-018-induced suppression of Ca^{2+} spiking in hippocampal neurons.

In low density hippocampal neurons, Ca^{2+} spiking was monitored before and after addition of different combinations of rimonabant and JWH-018. **(A)** For each drug combination evaluated, images were acquired from a minimum of 5 coverslips, from at least 2 different platings, with a minimum of 9 neuronal soma arbitrarily selected from each coverslip for determination of Ca^{2+} spiking frequency. The % frequency was calculated relative to the pre-drug condition within the individual coverslip. * $P < 0.05$ compared to the drug-free condition was determined using a one-way ANOVA and Dunnett's multiple comparison test. **(B)** Representative Ca^{2+} spiking profile

(static conditions) obtained from one coverslip to which JWH-018 (2.5 μM) was added. **(C)** Representative Ca^{2+} spiking profile (static conditions) obtained from one coverslip to which rimonabant (5 μM) and JWH-018 (2.5 μM) were added sequentially. For (B) and (C), vertical scale represents neuronal Fluo-4 fluorescence and horizontal scale represents time. Breaks in spiking represent pauses in signal acquisition to allow for addition of drug.

Fig. 6. (A) Phase contrast image of a hippocampal neuron culture grown on an MEA dish. (**B**) Typical raster plots from hippocampal neurons exposed to a 0.1 mM Mg^{2+} before (2 x 20 min recordings) and after (4 x 20 min recordings) addition of 10 μM 5F-PB-22. Regular synchronous neuronal firing detected from the majority of the 59 electrodes was almost entirely suppressed by 5F-PB-22.

Fig. 7. Effect of synthetic cannabinoids on spontaneous activity of hippocampal neurons grown on MEAs.

In cultured hippocampal neurons grown on MEAs, the % change in the number of spontaneous spikes was determined before and after addition of **(A)** 0.1% DMSO; **(B)** WIN 55,212-2 (10 and 1 μM); **(C)** WIN 55,212-3 (10 μM); **(D)** HU-210 (10 μM); **(E)** CP 55,940 (10 μM) and; **(F)** JWH-018 (10 and 1 μM). *N* equals ≥ 5 independent MEAs examined for each concentration. # $P < 0.05$, compared to DMSO using a 2-way ANOVA. * $P < 0.05$, compared to corresponding time point in DMSO using Bonferroni's multiple comparison test and 'ns' refers to not significantly different.

Fig. 8. Effect of ESCs on spontaneous activity of hippocampal neurons grown on MEAs.

In cultured hippocampal neurons grown on MEAs, the % change in the number of spontaneous spikes was determined before and after addition of **(A)** JWH-250 (10 and 1 μM); **(B)** XLR-11 (10 μM); **(C)** AB-PINACA (10 and 1 μM); **(D)** MAM-2201 (10 and 1 μM) and; **(E)** 5F-PB-22 (10 and 1 μM). *N* equals ≥ 5 independent MEAs examined for each concentration. # $P < 0.05$, compared to DMSO using a 2-way ANOVA. * $P < 0.05$, compared to corresponding time point in DMSO using Bonferroni's multiple comparison test and 'ns' refers to not significantly different.

Fig. 9. Effect of rimonabant on MAM-2201- and 5F-PB-22-induced suppression of spontaneous activity of hippocampal neurons grown on MEAs.

In cultured hippocampal neurons grown on MEAs, the % change in the number of spontaneous spikes was determined before and after addition of **(A)** the CB_1 antagonist rimonabant (5 μM);

no significant difference measured relative to time-matched effect of DMSO; **(B)** MAM-2201(5 μM) with or without rimonabant (5 μM); * significant difference between MAM-2201 and rimonabant for time-matched spiking and; **(C)** 5F-PB-22 (10 μM) with or without rimonabant (5 μM); # $P < 0.05$, comparison between groups using a 2-way ANOVA. * $P < 0.05$, comparison between corresponding time points using Bonferroni's multiple comparison test and 'ns' refers to not significantly different.

References

1. Atwood,B.K., Huffman,J., Straiker,A., Mackie,K., 2010. JWH018, a common constituent of 'Spice' herbal blends, is a potent and efficacious cannabinoid CB receptor agonist. Br.J Pharmacol. 160, 585-593. doi: 10.1111/j.1476-5381.2009.00582.x.

2. Bajo,M., Roberto,M., Schweitzer,P., 2009. Differential alteration of hippocampal excitatory synaptic transmission by cannabinoid ligands. J Neurosci Res. 87, 766-775. doi: 10.1002/jnr.21889

3. Blair,R.E., Deshpande,L.S., Sombati,S., Falenski,K.W., Martin,B.R., DeLorenzo,R.J., 2006. Activation of the cannabinoid type-1 receptor mediates the anticonvulsant properties of cannabinoids in the hippocampal neuronal culture models of acquired epilepsy and status epilepticus. J Pharmacol.Exp.Ther. 317, 1072-1078. doi: 10.1123/jpet.105.100354

4. Blau,A., Neumann,T., Ziegler,C., Benfenati,F., 2009. Replica-moulded polydimethylsiloxane culture vessel lids attenuate osmotic drift in long-term cell cultures. J Biosci. 34, 59-69.

5. Brents,L.K., Prather,P.L., 2014. The K2/Spice phenomenon: emergence, identification, legislation and metabolic characterization of synthetic cannabinoids in herbal incense products. Drug Metab Rev. 46, 72-85. doi: 10.3109/03602532.2013.839700

6. Cao,Z., Hammock,B.D., McCoy,M., Rogawski,M.A., Lein,P.J., Pessah,I.N., 2012. Tetramethylenedisulfotetramine alters Ca^{2+} dynamics in cultured hippocampal neurons: mitigation by NMDA receptor blockade and $GABA_A$ receptor-positive modulation. Toxicol.Sci. 130, 362-372. doi: 10.1093/toxsci/kfs244

7. Costain, W. J., Tauskela, J. S., Rasquinha, I., Comas, T., Hewitt, M, Marleau, V, and Soo, E. C. 2015. Pharmacological Characterization of Emerging Synthetic Cannabinoids in HEK293 Cells and Hippocampal Neurons. Submitted

8. Deshpande,L.S., Blair,R.E., Ziobro,J.M., Sombati,S., Martin,B.R., DeLorenzo,R.J., 2007. Endocannabinoids block status epilepticus in cultured hippocampal neurons. Eur.J Pharmacol. 558, 52-59. doi: 10.1016/j.ejphar.2006.11.030

9. Deshpande,L.S., Limbrick,D.D., Jr., Sombati,S., DeLorenzo,R.J., 2007. Activation of a novel injury-induced calcium-permeable channel that plays a key role in causing extended neuronal depolarization and initiating neuronal death in excitotoxic neuronal injury. J Pharmacol.Exp.Ther. 322, 443-452. doi: 10.1124/jpet.107.123182

10. Domenici,M.R., Azad,S.C., Marsicano,G., Schierloh,A., Wotjak,C.T., Dodt,H.U., Zieglgansberger,W., Lutz,B., Rammes,G., 2006. Cannabinoid receptor type 1 located on presynaptic terminals of principal neurons in the forebrain controls glutamatergic synaptic transmission. J Neurosci. 26, 5794-5799. doi: 10.1523/JNEUROSCI.0372-06.2006

11. Dunwiddie,T.V., Masino,S.A., 2001. The role and regulation of adenosine in the central nervous system. Annu.Rev.Neurosci. 24:31-55. doi: 10.1146/annurev.neuro.24.1.31

12. Glass,M., Northup,J.K., 1999. Agonist selective regulation of G proteins by cannabinoid CB_1 and CB_2 receptors. Mol.Pharmacol. 56, 1362-1369. doi: 10.1124/mol.56.6.1362

13. Hajos,N., Freund,T.F., 2002. Distinct cannabinoid sensitive receptors regulate hippocampal excitation and inhibition. Chem.Phys.Lipids. 121, 73-82. doi: 10.1016/S0009-3084(02)00149-4

14. Hoffman,A.F., Laaris,N., Kawamura,M., Masino,S.A., Lupica,C.R., 2010. Control of cannabinoid CB1 receptor function on glutamate axon terminals by endogenous adenosine acting at A_1 receptors. J Neurosci. 30, 545-555. doi: 10.1523/JNEUROSCI.4920-09.2010

15. Hoffman,A.F., Macgill,A.M., Smith,D., Oz,M., Lupica,C.R., 2005. Species and strain differences in the expression of a novel glutamate-modulating cannabinoid receptor in the rodent hippocampus. Eur.J Neurosci. 22, 2387-2391. doi: 10.1111/j.1460-9568.2005.04401.x

16. Ivenshitz,M., Segal,M., 2010. Neuronal density determines network connectivity and spontaneous activity in cultured hippocampus. J Neurophysiol. 104, 1052-1060. doi: 10.1152/jn.00914.2009

17. Jimbo,Y., Robinson,H.P., Kawana,A., 1993. Simultaneous measurement of intracellular calcium and electrical activity from patterned neural networks in culture. IEEE Trans.Biomed.Eng. 40, 804-810. doi: 10.1109/10.238465

18. Kang-Park,M.H., Wilson,W.A., Kuhn,C.M., Moore,S.D., Swartzwelder,H.S., 2007. Differential sensitivity of $GABA_A$ receptor-mediated IPSCs to cannabinoids in hippocampal slices from adolescent and adult rats. J Neurophysiol. 98, 1223-1230. doi: 10.1152/jn.00091.2007

19. Kawamura,Y., Fukaya,M., Maejima,T., Yoshida,T., Miura,E., Watanabe,M., Ohno-Shosaku,T., Kano,M., 2006. The CB1 cannabinoid receptor is the major cannabinoid receptor at excitatory presynaptic sites in the hippocampus and cerebellum. J Neurosci. 26, 2991-3001. doi: 10.1523/JNEUROSCI.4872-05.2006

20. Kelley,B.G., Thayer,S.A., 2004. Δ^9-tetrahydrocannabinol antagonizes endocannabinoid modulation of synaptic transmission between hippocampal neurons in culture. Neuropharmacology. 46, 709-715. doi: 10.1016/j.neuropharm.2003.11.005

21. Kofalvi,A., Vizi,E.S., Ledent,C., Sperlagh,B., 2003. Cannabinoids inhibit the release of [3H]glutamate from rodent hippocampal synaptosomes via a novel CB1 receptor-independent action. Eur.J Neurosci. 18, 1973-1978. doi:10.1046/j.1460-9568.2003.02897x

22. Kouznetsova,M., Kelley,B., Shen,M., Thayer,S.A., 2002. Desensitization of cannabinoid-mediated presynaptic inhibition of neurotransmission between rat hippocampal neurons in culture. Mol.Pharmacol. 61, 477-485. doi: 10.1124/mol.61.3.477

23. Kreitzer,F.R., Stella,N., 2009. The therapeutic potential of novel cannabinoid receptors. Pharmacol.Ther. 122, 83-96. doi: 10.1016/j.pharmthera.2009.01.005

24. Lauckner,J.E., Hille,B., Mackie,K., 2005. Lauckner,J.E., Hille,B., Mackie,K., 2005. The cannabinoid agonist WIN55,212-2 increases intracellular calcium via CB_1 receptor

coupling to $G_{q/11}$ G proteins. Proc.Natl.Acad.Sci.U.S.A. 102, 19144-19149. doi: 10.1073/pnas.0509588102

25. Leterrier,C., Laine,J., Darmon,M., Boudin,H., Rossier,J., Lenkei,Z., 2006. Constitutive activation drives compartment-selective endocytosis and axonal targeting of type 1 cannabinoid receptors. J Neurosci. 26, 3141-3153. doi: 10.1523/JNEUROSCI.5437-05.2006

26. Marsicano,G., Lutz,B., 1999. Expression of the cannabinoid receptor CB1 in distinct neuronal subpopulations in the adult mouse forebrain. Eur.J Neurosci. 11, 4213-4225. doi: 10.1046/j.1460-9568.1999.00847.x

27. Messer,R.D., Levine,E.S., 2012. Epileptiform activity in the CA1 region of the hippocampus becomes refractory to attenuation by cannabinoids in part because of endogenous gamma-aminobutyric acid type B receptor activity. J Neurosci Res. 90, 1454-1463. doi: 10.1002/jnr.23027

28. Nemeth,B., Ledent,C., Freund,T.F., Hajos,N., 2008. CB1 receptor-dependent and -independent inhibition of excitatory postsynaptic currents in the hippocampus by WIN 55,212-2. Neuropharmacology. 54, 51-57. doi: 10.1016/j.neuropharm.2007.07.003

29. Nicholson,R.A., Liao,C., Zheng,J., David,L.S., Coyne,L., Errington,A.C., Singh,G., Lees,G., 2003. Sodium channel inhibition by anandamide and synthetic cannabimimetics in brain. Brain Res. 978, 194-204. doi: 10.1016/S0006-8993(03)02808-7

30. Obrietan,K., van den Pol,A.N., 1999. GABAB receptor-mediated regulation of glutamate-activated calcium transients in hypothalamic and cortical neuron development. J Neurophysiol. 82, 94-102.

31. Ohno-Shosaku,T., Tsubokawa,H., Mizushima,I., Yoneda,N., Zimmer,A., Kano,M., 2002. Presynaptic cannabinoid sensitivity is a major determinant of depolarization-induced retrograde suppression at hippocampal synapses. J Neurosci. 22, 3864-3872.

32. Pacico,N., Mingorance-Le,M.A., 2014. New in vitro phenotypic assay for epilepsy: fluorescent measurement of synchronized neuronal calcium oscillations. PLoS.One. 9, e84755. doi: 10.1371/journal.pone.0084755

33. Pertwee,R.G., 2010. Receptors and channels targeted by synthetic cannabinoid receptor agonists and antagonists. Curr.Med.Chem. 17, 1360-1381.

34. Prather,P.L., Martin,N.A., Breivogel,C.S., Childers,S.R., 2000. Activation of cannabinoid receptors in rat brain by WIN 55212-2 produces coupling to multiple G protein alpha-subunits with different potencies. Mol.Pharmacol. 57, 1000-1010.

35. Rajasekaran,M., Brents,L.K., Franks,L.N., Moran,J.H., Prather,P.L., 2013. Human metabolites of synthetic cannabinoids JWH-018 and JWH-073 bind with high affinity and act as potent agonists at cannabinoid type-2 receptors. Toxicol.Appl.Pharmacol. 269, 100-108. doi: 10.1016/j.taap.2013.03.012

36. Ramirez-Franco,J., Bartolome-Martin,D., Alonso,B., Torres,M., Sanchez-Prieto,J., 2014. Cannabinoid type 1 receptors transiently silence glutamatergic nerve terminals of cultured cerebellar granule cells. PLoS.One. 9, e88594. doi: 10.1371/journal.pone.0088594

37. Seely,K.A., Lapoint,J., Moran,J.H., Fattore,L., 2012. Spice drugs are more than harmless herbal blends: a review of the pharmacology and toxicology of synthetic cannabinoids. Prog.Neuropsychopharmacol.Biol.Psychiatry. 39, 234-243. doi: 10.1016/j.pnpbp.2012.04.017.

38. Shen,M., Piser,T.M., Seybold,V.S., Thayer,S.A., 1996. Cannabinoid receptor agonists inhibit glutamatergic synaptic transmission in rat hippocampal cultures. J Neurosci. 16, 4322-4334.

39. Shen,M., Thayer,S.A., 1998a. Cannabinoid receptor agonists protect cultured rat hippocampal neurons from excitotoxicity. Mol.Pharmacol. 54, 459-462. doi: 10.1124/mol.54.3.459

40. Shen,M., Thayer,S.A., 1998b. The cannabinoid agonist Win55,212-2 inhibits calcium channels by receptor-mediated and direct pathways in cultured rat hippocampal neurons. Brain Res. 783, 77-84. doi: 10.1016/S0006-8993(97)01195-5

41. Shen,M., Thayer,S.A., 1999. Δ^9-tetrahydrocannabinol acts as a partial agonist to modulate glutamatergic synaptic transmission between rat hippocampal neurons in culture. Mol.Pharmacol. 55, 8-13. doi: 10.1124/mol.55.1.8

42. Sousa,V.C., Assaife-Lopes,N., Ribeiro,J.A., Pratt,J.A., Brett,R.R., Sebastiao,A.M., 2011. Regulation of hippocampal cannabinoid CB_1 receptor actions by adenosine A_1 receptors and chronic caffeine administration: implications for the effects of Δ^9-tetrahydrocannabinol on spatial memory. Neuropsychopharmacology. 36, 472-487. doi: 10.1038/npp.2010.179

43. Steindel,F., Lerner,R., Haring,M., Ruehle,S., Marsicano,G., Lutz,B., Monory,K., 2013. Neuron-type specific cannabinoid-mediated G protein signalling in mouse hippocampus. J Neurochem. 124, 795-807. doi: 10.1111/jnc.12137

44. Sullivan,J.M., 1999. Mechanisms of cannabinoid-receptor-mediated inhibition of synaptic transmission in cultured hippocampal pyramidal neurons. J Neurophysiol. 82, 1286-1294.

45. Takahashi,K.A., Castillo,P.E., 2006. The CB1 cannabinoid receptor mediates glutamatergic synaptic suppression in the hippocampus. Neuroscience. 139, 795-802. doi: 10.1016/j.neuroscience.2006.01.024

46. Tauskela,J.S., Brunette,E., Monette,R., Comas,T., Morley,P., 2003. Preconditioning of cortical neurons by oxygen-glucose deprivation: tolerance induction through abbreviated neurotoxic signaling. Am.J.Physiol Cell Physiol 285, C899-C911. doi: 10.1152/ajpcell.00110.2003

47. Twitchell,W., Brown,S., Mackie,K., 1997. Cannabinoids inhibit N- and P/Q-type calcium channels in cultured rat hippocampal neurons. J Neurophysiol. 78, 43-50.

48. Wagenaar,D.A., Pine,J., Potter,S.M., 2006. An extremely rich repertoire of bursting patterns during the development of cortical cultures. BMC.Neurosci. 7:11. doi: 10.1186/1471-2202-7-11

49. Wiley,J.L., Marusich,J.A., Huffman,J.W., Balster,R.L., Thomas,B.F., 2011. Hijacking of Basic Research: The Case of Synthetic Cannabinoids. Methods Rep.RTI.Press. 2011. 17971. doi: 10.3768/rtipress.2011.op.0007.1111

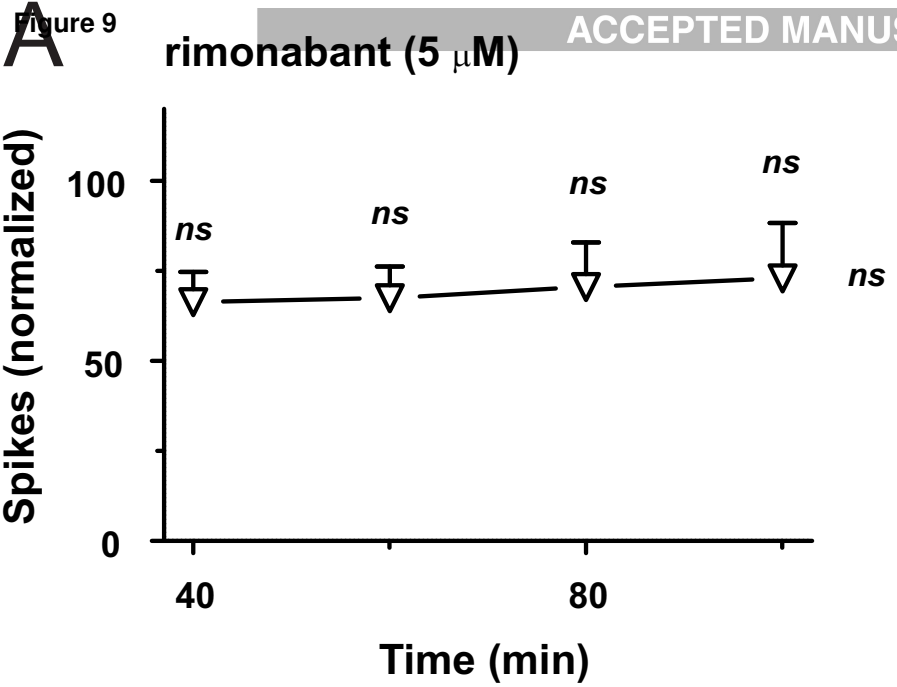

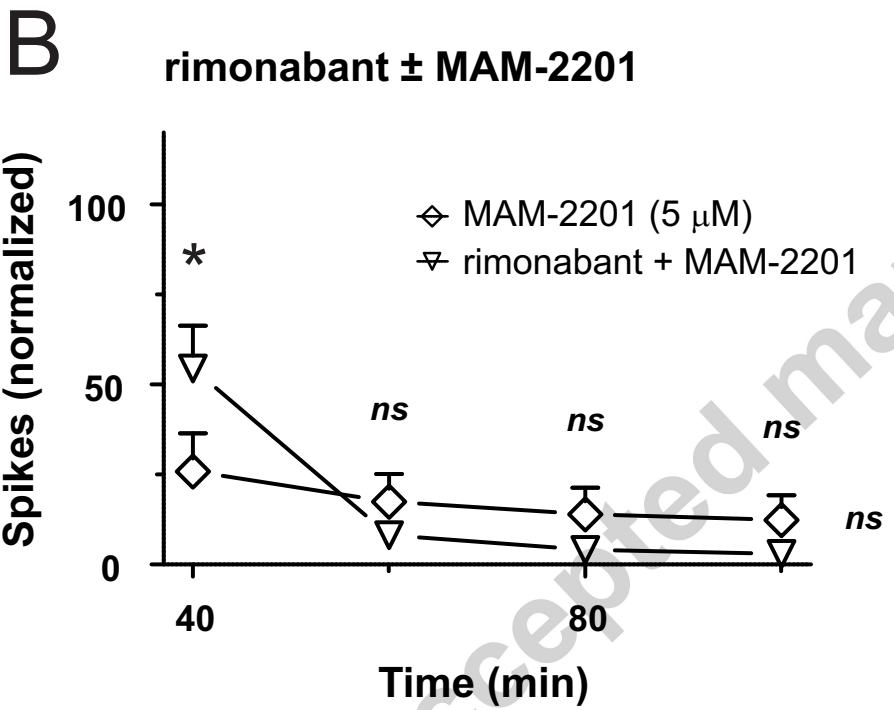

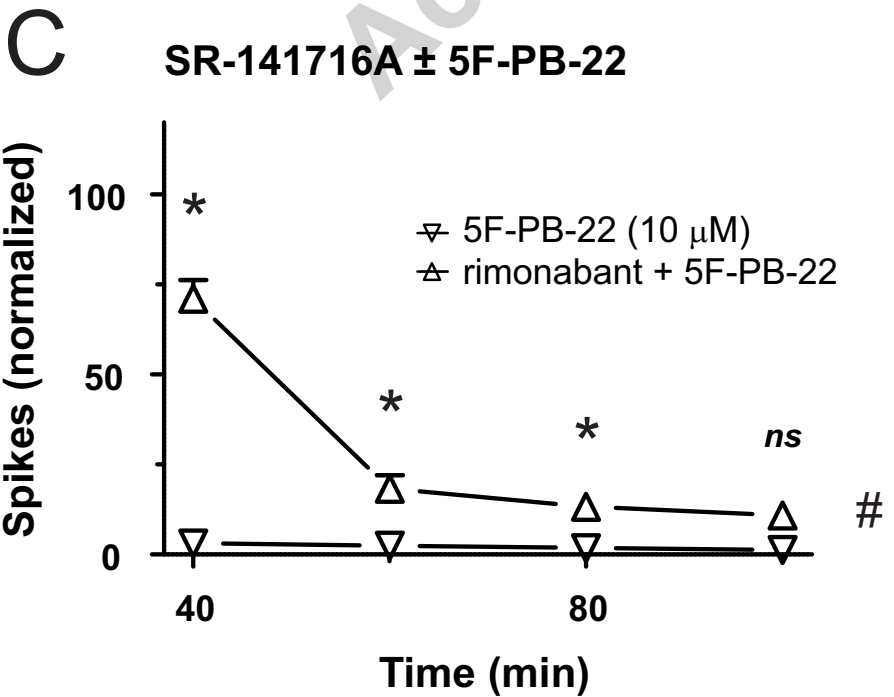

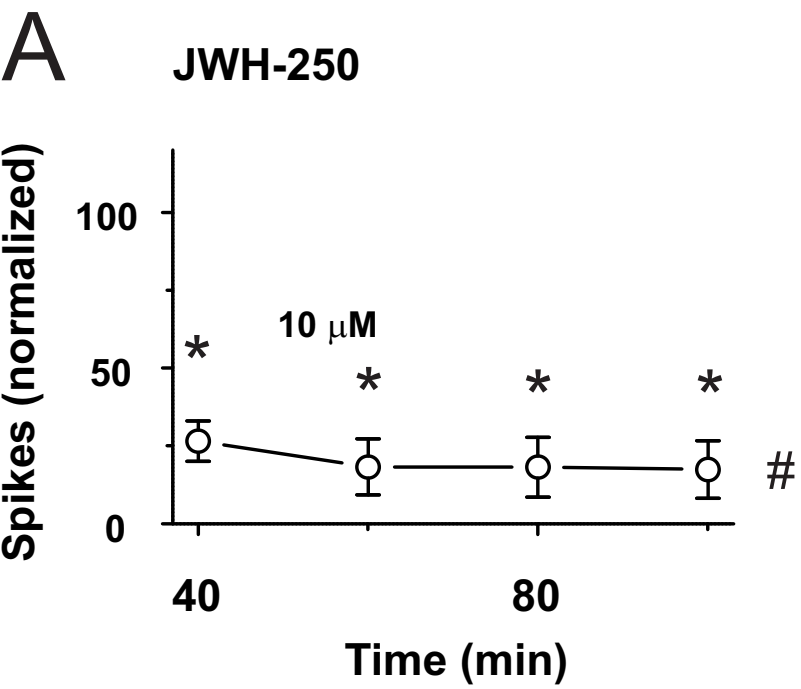

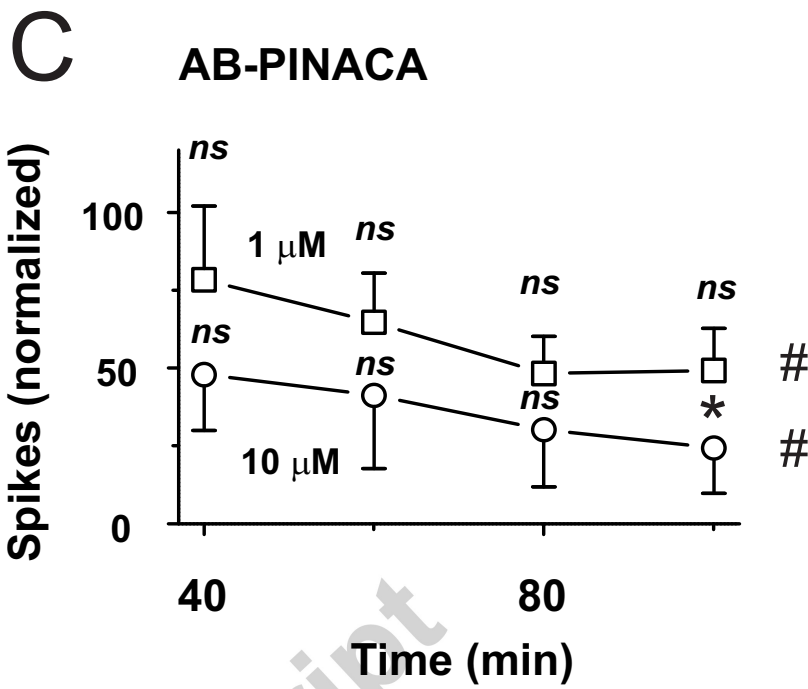

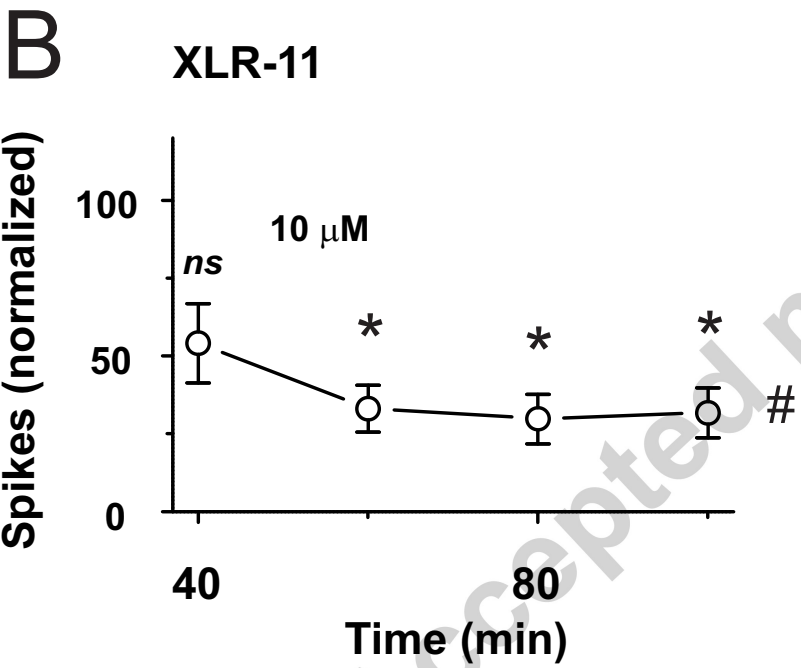

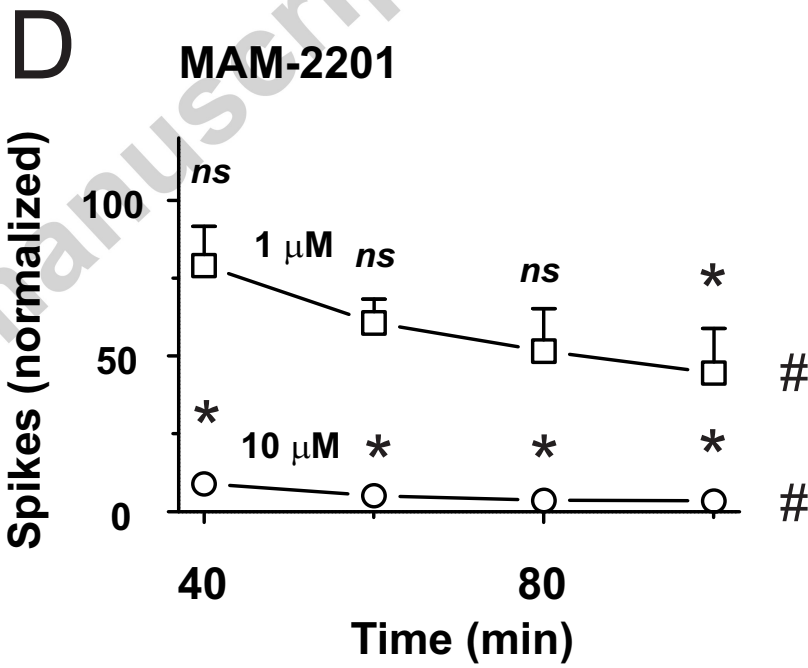

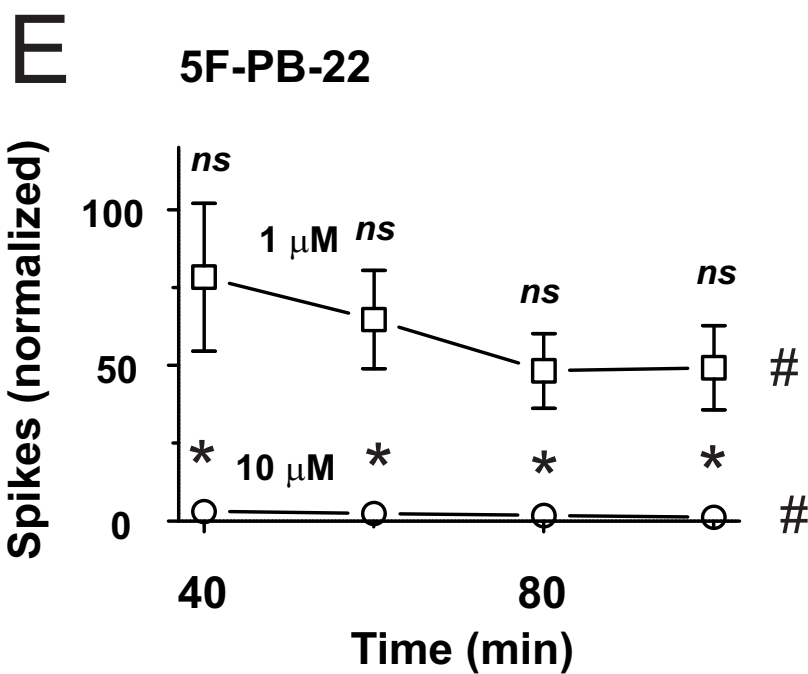

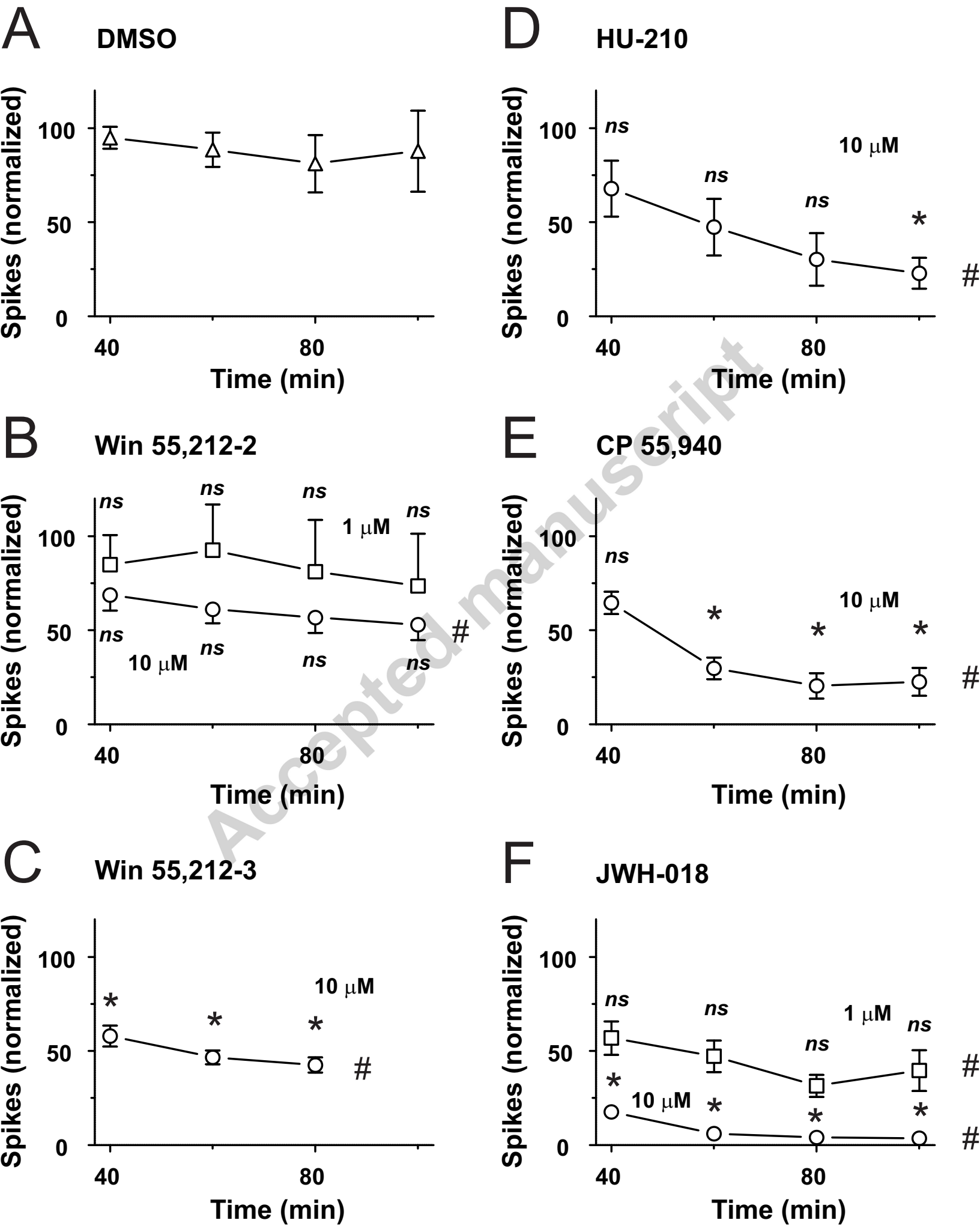

Figure 6

Click here to download high resolution image

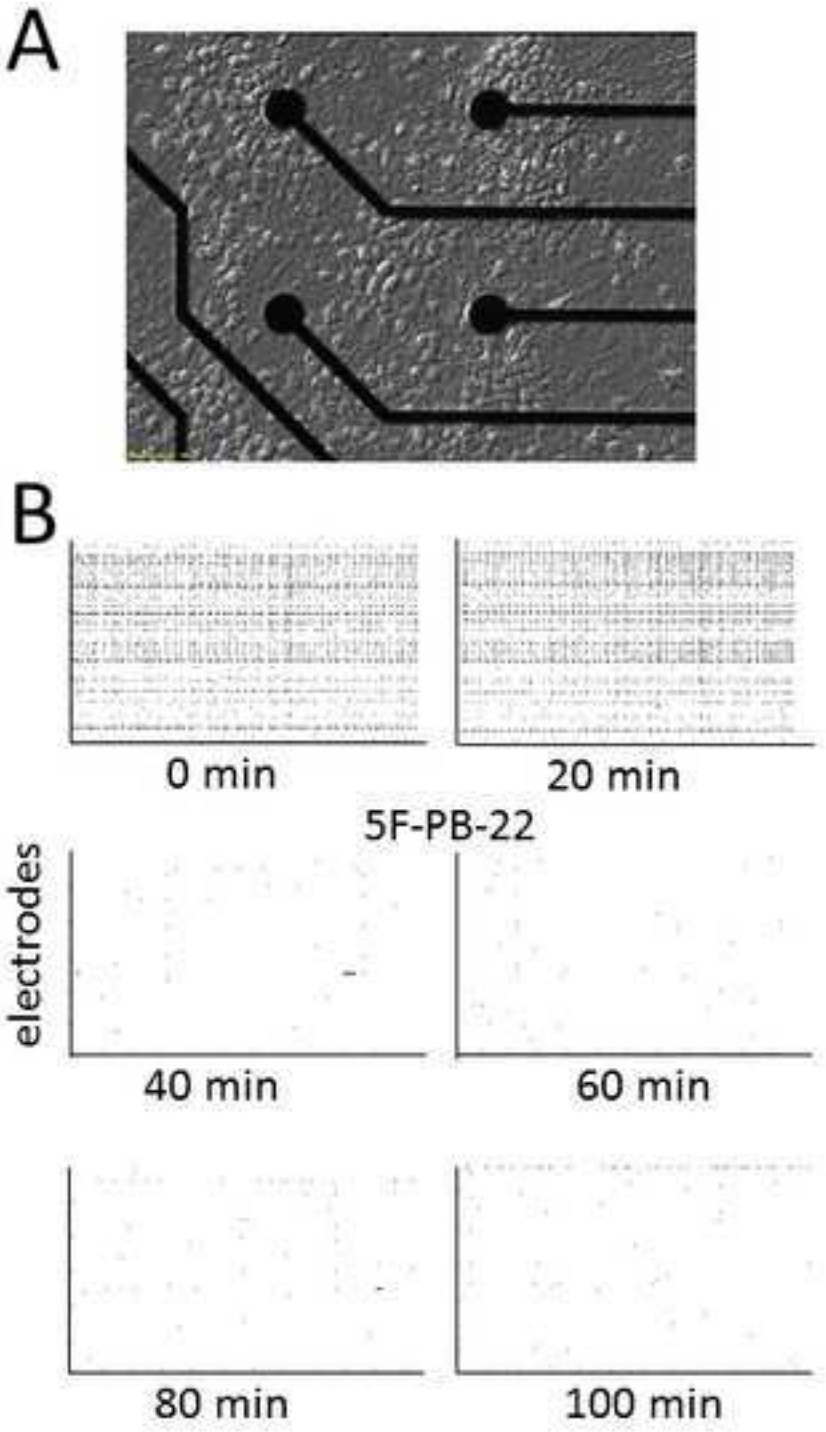

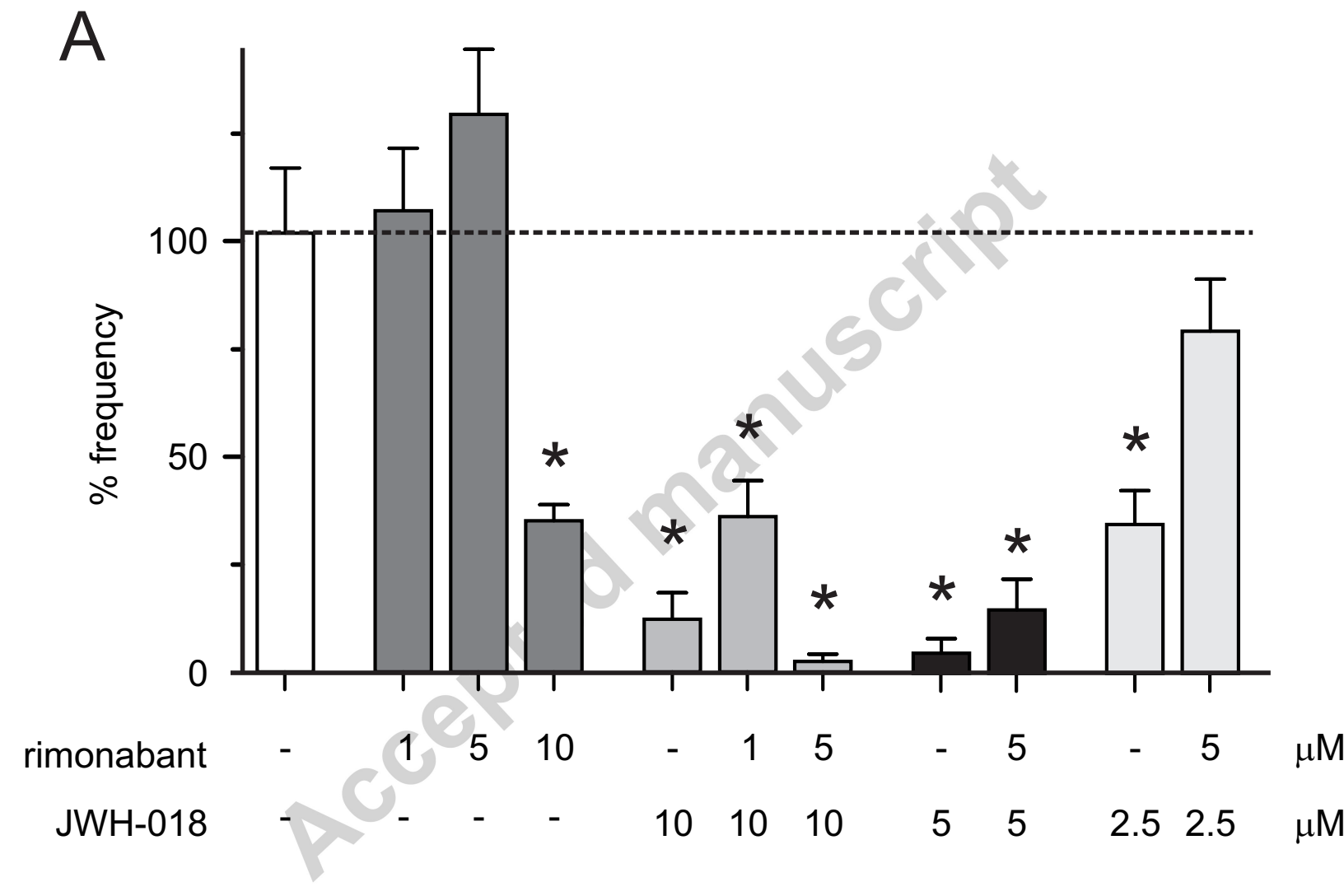

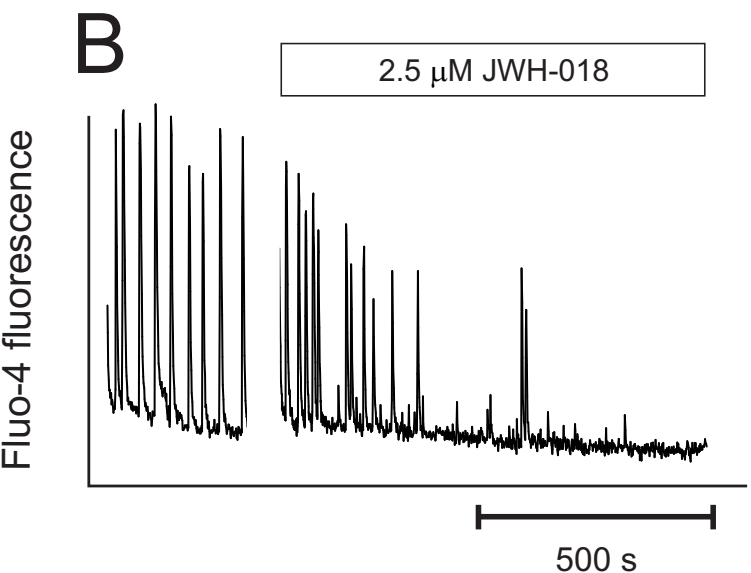

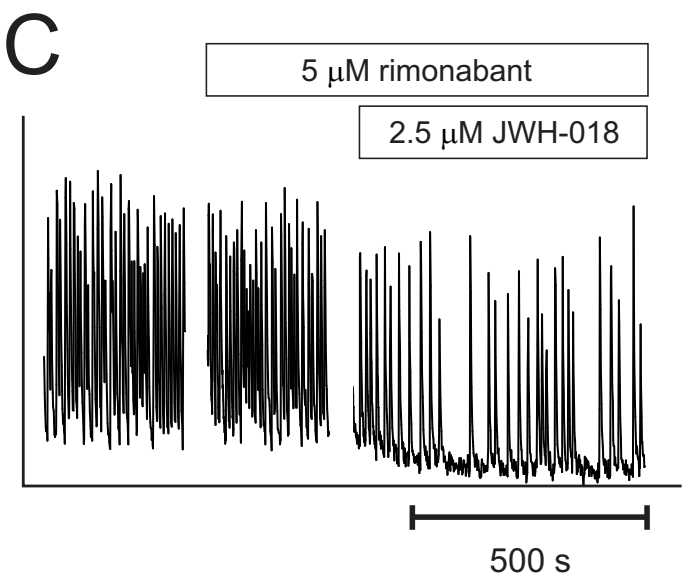

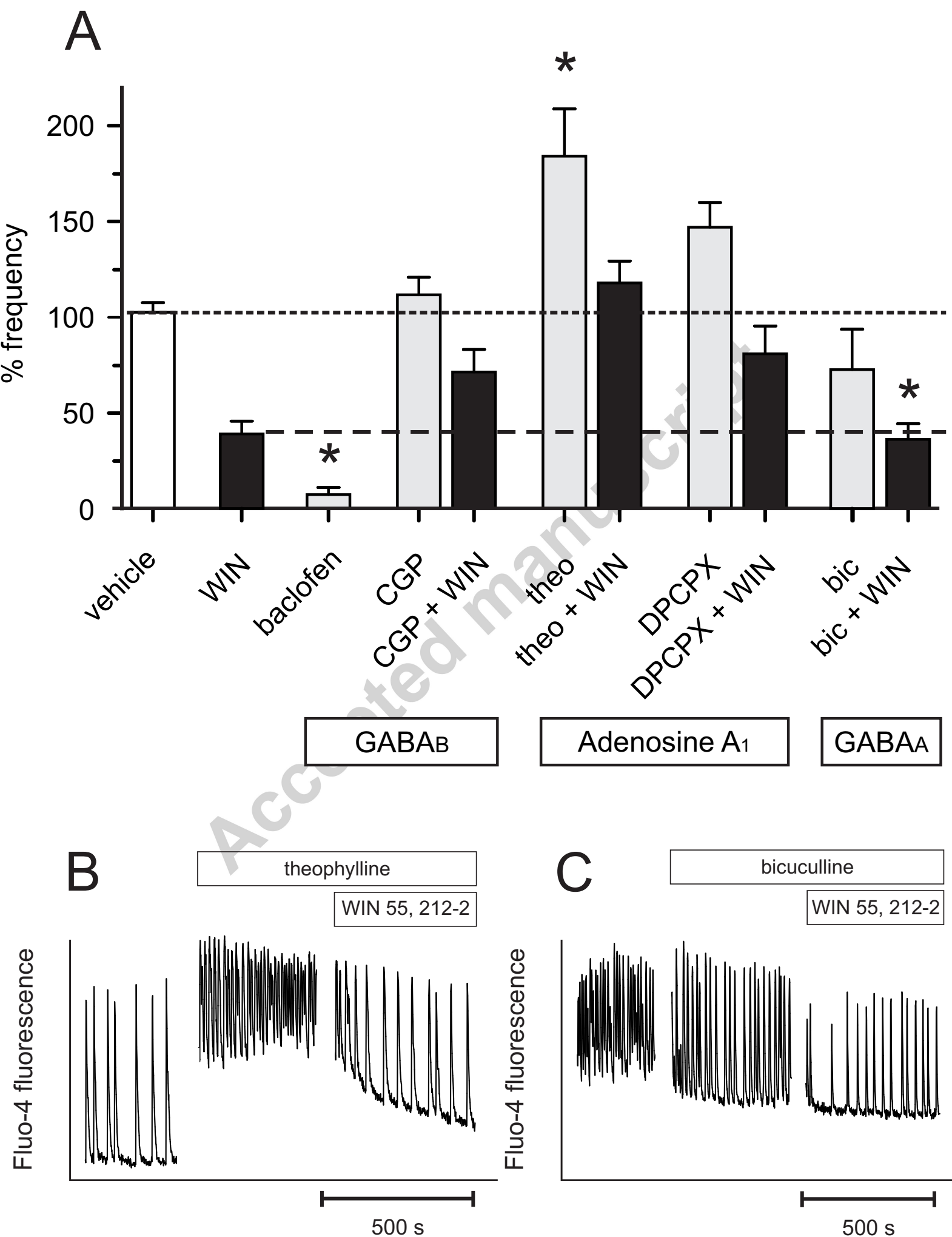

A(i)

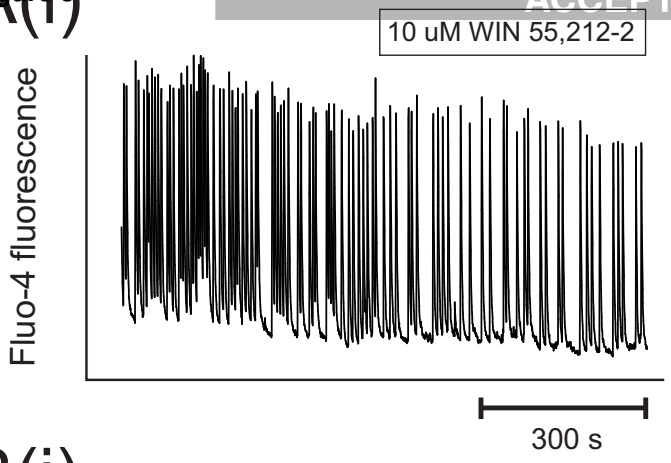

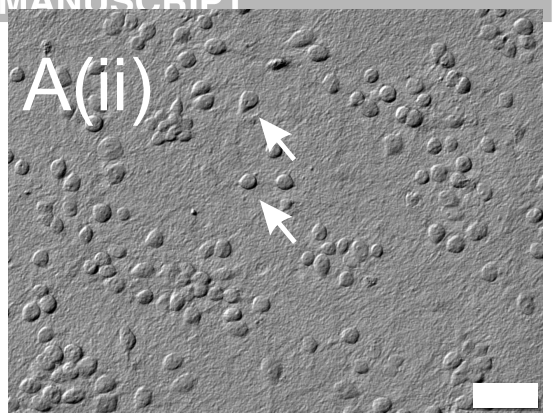

hippocampal, high density, perfused

B(i)

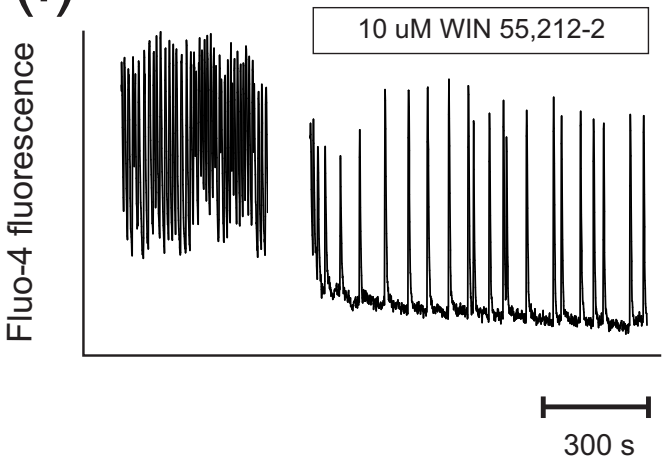

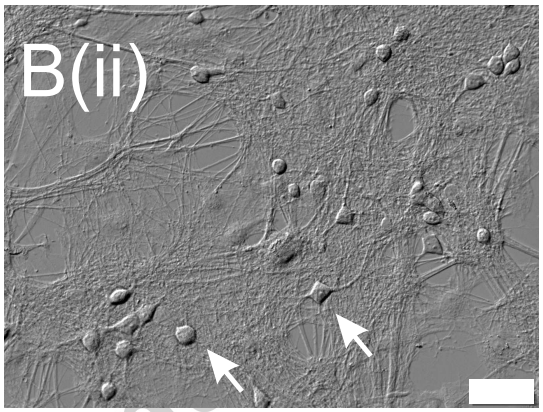

hippocampal, low density, static

C(i)

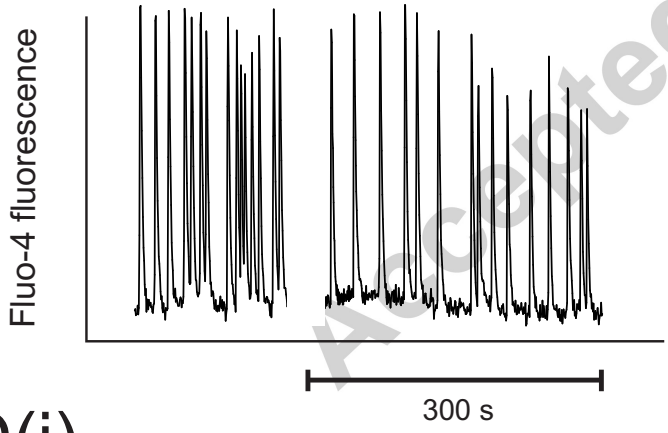

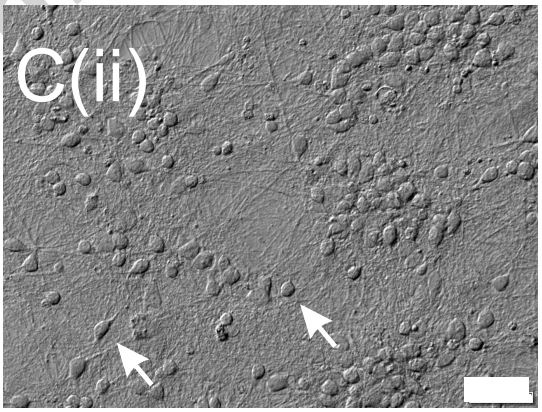

cortical, high density, static

D(i)

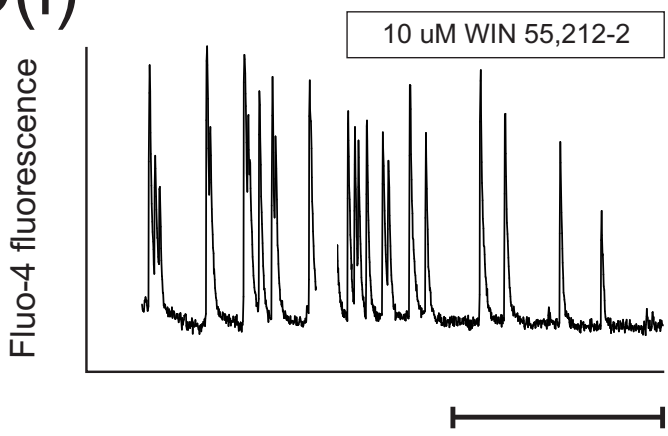

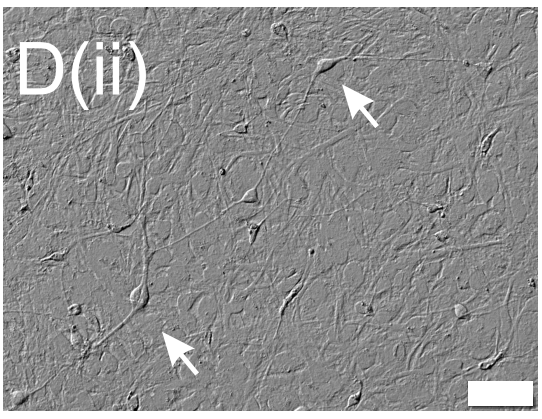

hippocampal (very low density) on pre-established astrocytes, static

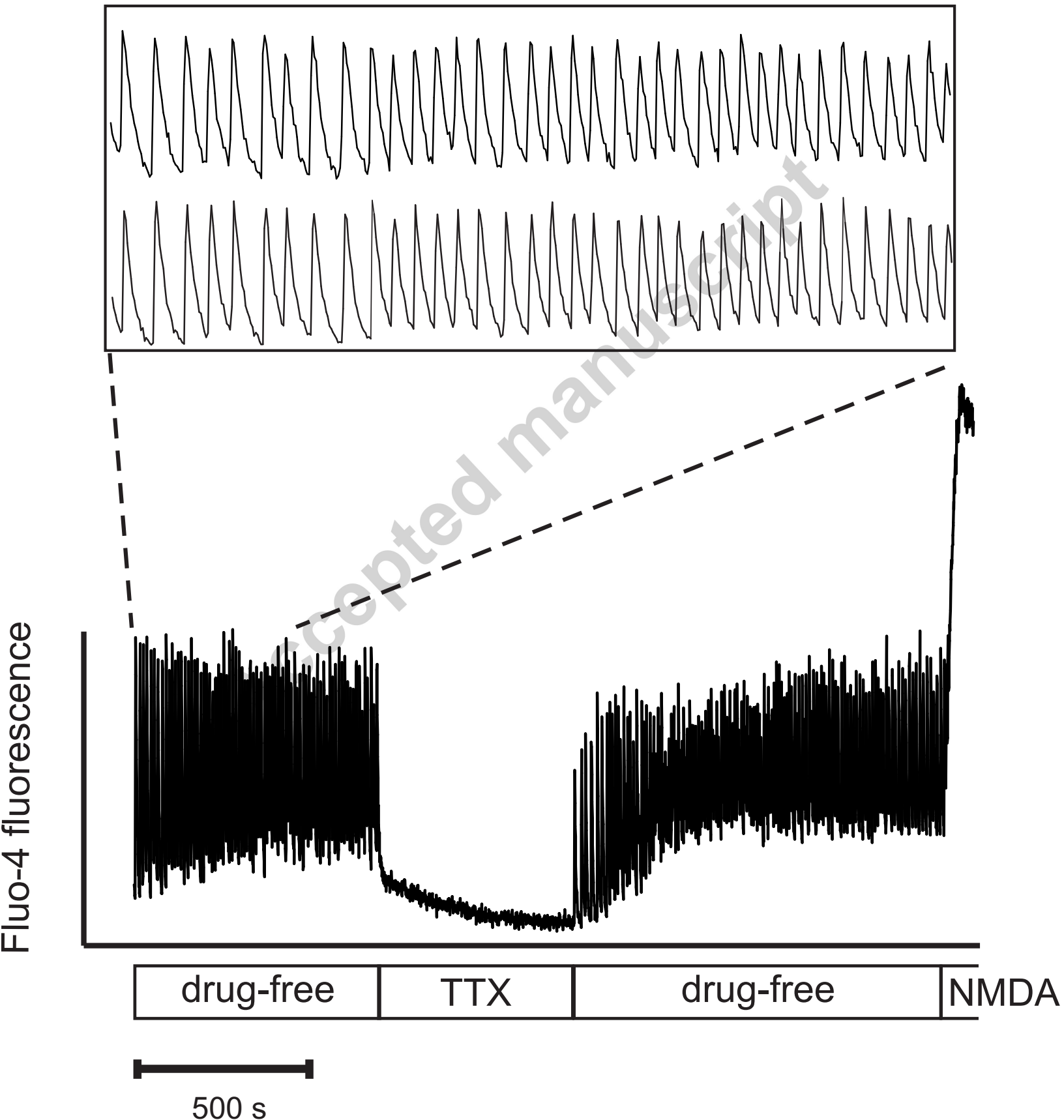

Figure 1